Physics of the Earth and Planetary Interiors 178 (2010) 2–7

Contents lists available at ScienceDirect

Physics of the Earth and Planetary Interiors

journal homepage: www.elsevier.com/locate/pepi

Ab initio lattice dynamics calculations on the combined effect of temperature and silicon on the stability of different iron phases in the Earth's inner core

Alexander S. Côté*, Lidunka Vočadlo, David P. Dobson, Dario Alfè, John P. Brodholt

Department of Earth Sciences, University College London, Gower Street, London WC1E 6BT, United Kingdom

ARTICLE INFO

Article history:
Received 31 January 2009
Received in revised form 16 May 2009
Accepted 1 July 2009

Keywords:
Earth's inner core
Iron alloys
Silicon
Lattice dynamics
Ab initio calculations
Crystal structure

ABSTRACT

The Earth's solid inner core consists mainly of iron (Fe), alloyed with lighter elements, such as silicon (Si). Interpretation of seismic anisotropy and layering requires knowledge of the stable crystal structure in the inner core. We report ab initio density functional theory calculations on the free energy and vibrational stability of pure iron and Fe–Si alloys at conditions representative of the Earth's inner core. For pure Fe the stable phase is already known to be hexagonal close-packed (hcp). However, with the addition of ~7 wt.% Si at high temperatures, we observe a transition to the face-centred cubic (fcc) phase. We also produce a phase diagram for the Fe–Si system and show that the inner core may exist in the two-phase region, with coexisting fcc and hcp. This may also explain the low S-velocities observed in the inner core.

1. Introduction

Constraining the crystalline phase in the inner core has a long history (e.g. Anderson, 1985; Boehler, 1986; Saxena et al., 1993; Saxena and Dubrovinsky, 2000; Stixrude and Cohen, 1995; Andrault et al., 1997; Alfè et al., 2000a,b; Lin et al., 2002; Vočadlo et al., 1997, 1999, 2003; Belonoshko et al., 2003, 2008; Dubrovinsky, 2007; Côté et al., 2008a,b). Under ambient conditions, the iron crystal has a body-centred cubic (bcc) structure. Increasing temperature at ambient pressure causes a transformation to the face-centred cubic (fcc) phase above ~1150 K. At pressures above ~11 GPa (at room temperature), it adopts a hexagonal close-packed (hcp) structure which persists to Earth's inner core pressures. Pure Fe in the bcc phase was previously excluded as a possible crystal structure in the core, because it is mechanically unstable at high pressures (Stixrude et al., 1994; Söderlind et al., 1996). However, the effect of temperature has proven to be very important, and the stable phase at core pressures and temperatures remains ambiguous. High temperature has been shown to decrease the free energy difference between bcc and hcp phases (Vočadlo et al., 2003), and molecular dynamics calculations have found bcc to be mechanically stable at core conditions (Belonoshko et al., 2003; Vočadlo et al., 2003). Recently the face-centred cubic (fcc) phase was proposed as a third possible structure in the inner core, with a free energy between those of bcc and hcp (Vočadlo et al., 2008). Since the core is likely to be an iron alloy, the effect of alloying elements on the crystal structure has to be considered. In a previous ab initio study we showed that at core pressure and zero temperature, light elements (Si, S, C, O) tend to stabilise the bcc phase with respect to hcp, but hcp still remains the most stable phase (Côté et al., 2008a,b). Here we present the results of ab initio lattice dynamics (LD) calculations, to evaluate the effect of temperature on the crystal structure of iron and Fe–Si alloys at core pressures.

2. Computational methods

The density functional theory (DFT) calculations in this work were carried out using the VASP code (Kresse and Furthmuller, 1996), which incorporates the projected augmented wave (PAW) method (Blöchl, 1994). The exchange-correlation energy was represented by the generalised gradient approximation (GGA) (Wang and Perdew, 1991). VASP calculates the ground state ($T = 0$) for each set of ionic positions and the electronic free energy is taken as the quantity to be minimised. Care was taken when choosing the k-point sampling grid and cutoff energies in order to have an energy convergence of no more than 1 meV/atom. Specifically, we used a 400 eV cutoff energy throughout the calculations. For pure iron bcc and fcc in the 2-atom cells, $12 \times 12 \times 12$ (equivalent to 56 k-points in the irreducible Brillouin zone (IBZ)) and $12 \times 12 \times 8$ (84 k-points in the IBZ) k-point grids were used respectively. For hcp a 4-atom cell was used, with a $15 \times 9 \times 9$ grid (200 k-points in the IBZ). Larger primitive cells (8–16 atoms) were used for the alloyed structures, and correspondingly smaller k-point sampling grids.

* Corresponding author. Tel.: +44 020 7679 2425; fax: +44 020 7679 2685.
E-mail address: a.cote@ucl.ac.uk (A.S. Côté).

0031-9201/$ – see front matter © 2009 Elsevier B.V. All rights reserved.
doi:10.1016/j.pepi.2009.07.004

We calculated the phonon frequencies for different structures and examined their vibrational stability. The phonon calculations were carried out using the code PHON (Alfè, 2009), which uses the small displacement method to construct force-constant matrices. The force-constant matrix $\mathbf{\Phi}_{is\alpha,jt\beta}$ is the central quantity in the calculation of the phonon vibrational frequencies, since the (squares of the) frequencies at wavevector $\mathbf{k}$ are the eigenvalues of the dynamical matrix $D_{s\alpha,t\beta}$, defined as

$$\mathbf{D}_{s\alpha,\,t\beta}(\mathbf{k}) = \frac{1}{\sqrt{M_s M_t}} \sum_i \mathbf{\Phi}_{is\alpha,jt\beta} \exp\left[i\mathbf{k}\cdot(\mathbf{R}_j^0 + \tau_t - \mathbf{R}_i^0 - \tau_s)\right] \quad (1)$$

where $\mathbf{R}_i^0$ is a vector of the lattice connecting different primitive cells and τ_s is the position of the atom s in the primitive cell. If we have the complete force-constant matrix, then $\mathbf{D}_{s\alpha,\,t\beta}$ and hence the frequencies $\omega_{s\mathbf{k}}$ can be obtained at any $\mathbf{k}$. In principle, the elements of $\mathbf{\Phi}_{is\alpha,jt\beta}$ are nonzero for arbitrarily large separations $\left|\mathbf{R}_j^0 + \tau_t - \mathbf{R}_i^0 - \tau_s\right|$, but in practice they decay rapidly with separation, so PHON neglects all the elements beyond a certain cutoff distance resulting in a force-constant matrix of finite extent.

Our calculations were extended to nonzero temperatures by using the quasi-harmonic approximation, where the volume and temperature dependence of the Helmholtz free energy $F(V,T)$ was calculated as a sum of the contributions due to static compression, $F_0(V)$, thermal excitation of electrons, $F_{el}(V,T)$ and thermal excitation of phonons, $F_{vib}(V,T)$:

$$F(V,T) = F_0(V) + F_{el}(V,T) + F_{vib}(V,T) \quad (2)$$

The last term in (2) is defined as

$$F_{vib}(V,T) = k_B T \sum_{s,\mathbf{k}} \ln\left[2\,\sinh\left(\frac{h\omega_{s\mathbf{k}}}{2k_B T}\right)\right] \quad (3)$$

where k_B is the Boltzman constant, and $\omega_{s\mathbf{k}}$ is the frequency of the phonon mode for wave vector $\mathbf{k}$ and volume V.

The contribution to the free energy from electronic excitations at different electronic temperatures $F_{el}(V,T)$ was included by using a Fermi smearing function when calculating the ground-state energy in VASP.

The Gibbs free energy was then obtained by

$$G(P,T) = F(V,T) + PV \quad (4)$$

In order to account for the contribution of thermal pressure at different temperatures and obtain the last term of (4) accurately, we performed free energy calculations at 6 different volumes, corresponding to pressures in the range of 200–400 GPa. We then fitted the results to an $E(V)$ equation of state, from where we were able to find the correct volume for any pressure at various temperatures. The total free energies for core pressures and temperatures could thus be evaluated.

It should be noted that the calculations are quasi-harmonic and, therefore, neglect anharmonicity. The melting temperature of Fe under core pressures is about 6000 K so anharmonicity may start to become important after about 4000 K or so. However, the total anharmonic contribution to the free energy of hcp Fe at 6000 K is only of the order of 60 meV/atom (Alfè et al., 2001). Since fcc is a close-packed structure like hcp, it should be affected by anharmonicity in a similar way. It is thus unlikely for the free energy differences to be larger than 10 meV/atom or so, even at very high temperatures. BCC, however, is not close packed, and so the anharmonic contribution to the free energy may be higher.

3. Results

3.1. Vibrational stability

To get accurate results in the harmonic approximation, very accurate forces are needed. We therefore used a very low tolerance criterion for the total energy (10^{-7} eV), and an added grid in the Fourier transform mesh which serves to reduce the noise in the forces, which were set to converge below 10^{-5} eV/Å. The atoms were displaced a small distance (0.01 Å) from their equilibrium positions, in order for the forces to remain within the harmonic approximation, and the forces were calculated. For all cases, the calculations were performed on supercells large enough to avoid self-interaction due to the periodic boundary conditions, typically 3 times the size of the primitive unit cell in each direction. The resulting supercells contained up to 288 atoms.

Firstly we calculated phonon frequencies for pure Fe at different pressures and electronic temperatures. The calculated dispersion relations for bcc Fe for certain special directions of the 1st Brillouin zone are displayed in Fig. 1.

As reported previously (Vočadlo et al., 2003), at low temperatures the bcc phase (Fig. 1a) becomes vibrationally unstable at high pressures above ~200 GPa. Furthermore, as can be seen from Fig. 1b, at pressures below 250 GPa, high electronic temperatures contribute to destabilising the structure. This is manifested in a soft mode in the [1 1 0] (M-Γ) direction, which starts from zero pressure, and is due to bcc transforming to the fcc phase. Approaching core pressures, high temperatures do act towards eliminating some imaginary frequencies in certain directions and stabilising the structure, but overall the bcc phase remains dynamically unstable. High pressures in combination with electronic excitations at high temperatures also act to suppress magnetic moments, and this was confirmed by spin polarised calculations in this work, as well as in previous studies (Vočadlo et al., 2003).

The hcp and fcc phases of pure iron are both dynamically stable at core pressures, and the phonon dispersion relations at T_{el} = 5500 K and 330 GPa are presented in Fig. 2.

We then substitutionally inserted small concentrations of silicon at high pressure in all three phases. As can be seen in Fig. 3, the imaginary frequencies in the bcc phase disappear with increasing Si concentration, making the Fe–Si alloy vibrationally stable at 10.4 wt.% (12.5 at.%) and above. This is consistent with the experimental results for FeSi, where a bcc (B2) structure is stable at core conditions (Dobson et al., 2002). In contrast, we find that increasing Si concentration destabilises the hcp structure; at 25 at.% Si, hcp is completely unstable. It should be noted that in the alloyed structure, magnetic moments disappear with high pressure even at low temperatures.

3.2. Thermodynamical stability

To compare the thermodynamical stability of bcc, hcp and fcc we used a 10.4 wt.% iron–silicon alloy (3 Si atoms and 13 Fe atoms), a concentration at which all three structures are vibrationally stable. As there is more than one possible Si defect, a number of trials were performed with all the different configurations of the defect atoms in all phases, and the most favourable configurations at high pressure were chosen. They are shown in Fig. 4. The Gibbs free energy vs. temperature at a pressure of 330 GPa is plotted in Fig. 5, relative to the hcp phase.

It is clear that the free energy difference between hcp and the other two phases diminishes significantly with increasing temperature. The free energy difference between hcp and bcc with 10.4 wt.% Si reduces to only 36 meV/atom at 330 GPa and 5500 K, although the free energies are still in favour of hcp. More interestingly, fcc becomes the most stable structure at temperatures above 4000 K.

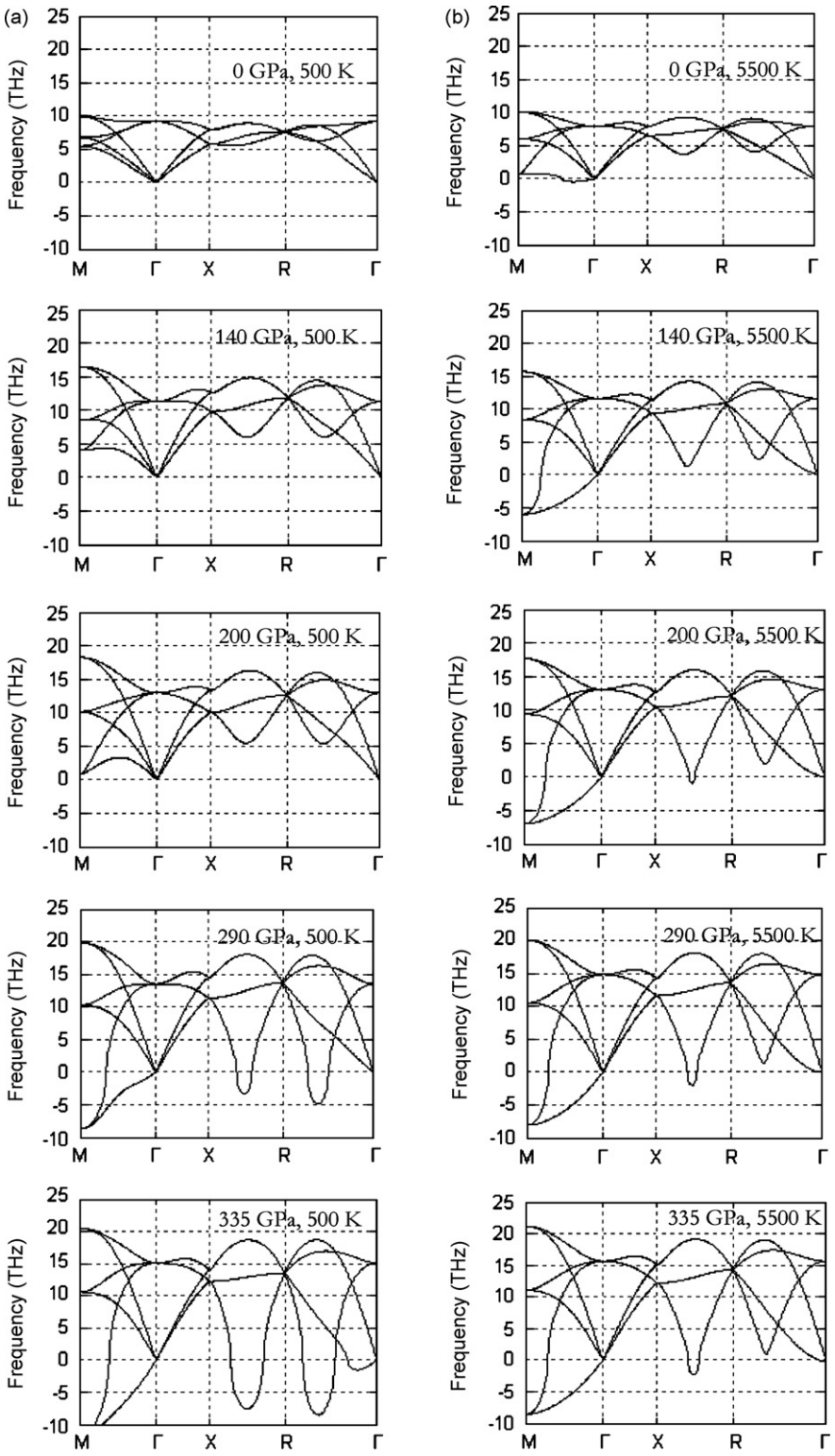

Fig. 1. Phonon dispersion relations of pure bcc Fe at (a) 500 K and (b) 5500 K, and a range of pressures. It can be seen that temperature has an important effect on the structure's vibrational stability. At relatively low temperatures, pressure is the main stability factor, but that changes at core temperatures. At inner core conditions, high temperature acts towards stabilising the structure. Magnetism was included in all the pure iron calculations.

We then focused on hcp and fcc – thermodynamically the most stable structures – at three different Si concentrations, 3.2 wt.%, 6.7 wt.% and 10.4 wt.%. We repeated the phonon calculation for all concentrations and derived the free energies. We can see from Fig. 6 that as the Si concentration increases, fcc becomes the most stable phase at concentrations greater than ~7 wt.% (~13 at.%), at inner core pressures and temperatures.

Fig. 6 represents the pseudounivariant at 5500 K, where one phase directly transforms into the other, but in reality the two phases would mix to form a solid solution. Thus, the free energy of

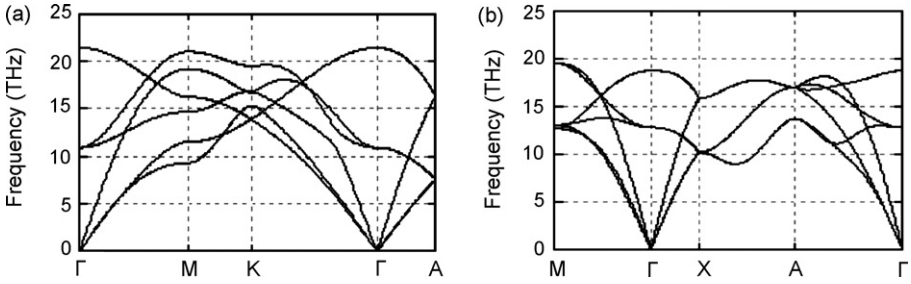

Fig. 2. Phonon dispersion of (a) hcp and (b) fcc phases of pure iron at Earth's inner core conditions.

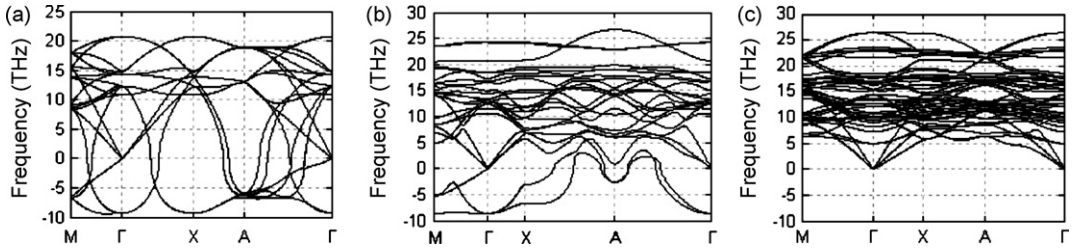

Fig. 3. Phonon dispersion relations for the bcc phase at 330 GPa for (a) pure iron, (b) 6.7 wt.% Si, and (c)10.4 wt.% Si. For this calculation no electronic temperature was used. It is clear that the addition of Si vibrationally stabilises the structure.

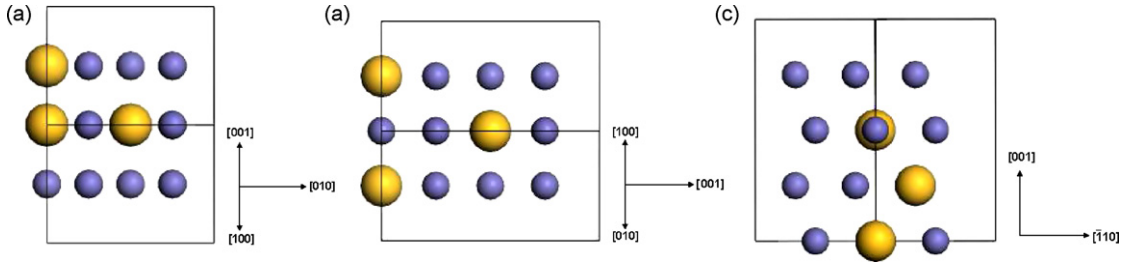

Fig. 4. The most stable configurations used for (a) bcc, viewed along ⟨1 0 1⟩, (b) fcc, viewed along ⟨1 1 0⟩, and (c) hcp, viewed along ⟨1 1 0⟩. The periodic boundary conditions are not shown. The substituted silicon atoms are enlarged for clarity.

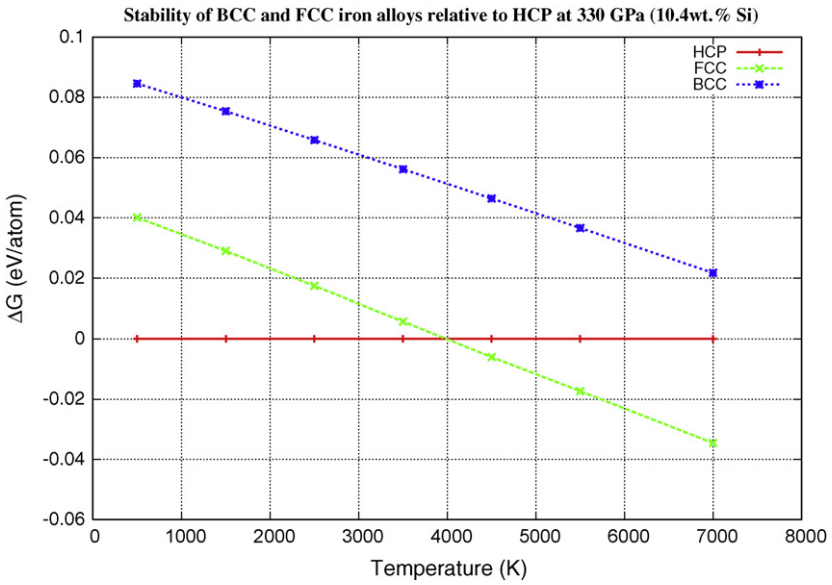

Fig. 5. Relative Gibbs free energies of the bcc and fcc structures with respect to hcp, at 330 GPa. Increasing temperature decreases the energy difference, and above 4000 K, fcc becomes the most stable structure at the 10.4 wt.% Si concentration.

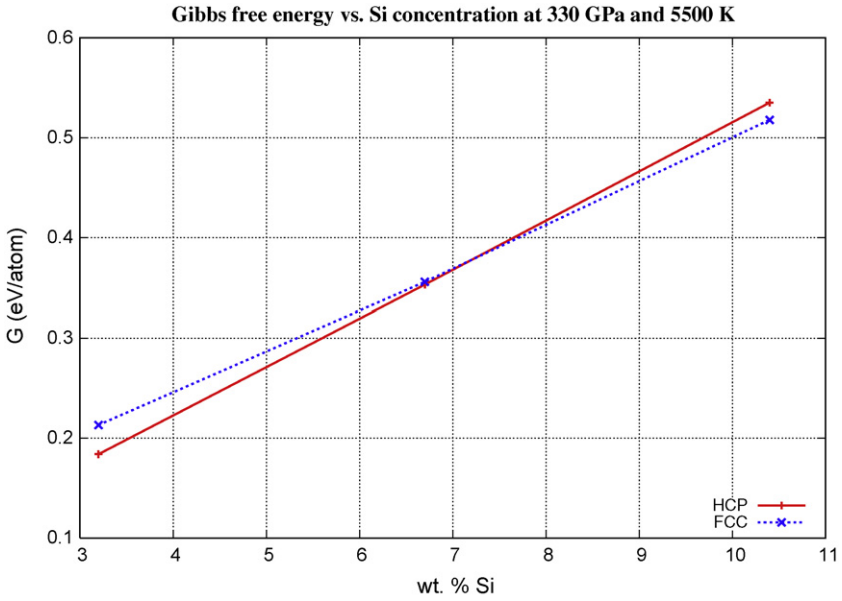

Fig. 6. Gibbs free energy of fcc and hcp at Earth's inner core conditions, relative to pure hcp Fe. At Si concentrations above 7 wt.% (13 at.%), fcc is found to be the most stable structure thermodynamically.

the solid solution was derived by adding the configurational term $k_B T(c_{Si}\ln(c_{Si}) + c_{Fe}\ln(c_{Fe}))$ to the energies of the individual phases, where c represents the atomic % concentration. The solid solution energies were then fitted to a polynomial for different concentrations, and by taking the common tangent of the two curves, the coexisting compositions of the fcc and hcp phases were calculated. Using these, we derived an approximate phase diagram for the Fe–Si system, shown in Fig. 7, for 330 GPa and 360 GPa. Also plotted in Fig. 7 are the Fe–Si solid solution melting temperatures and compositions, predicted by Alfè et al. (2002). Note that the narrow width of our predicted two-phase region is completely consistent with the narrow solid solution melting curve inferred from Alfè et al.'s results. The phase diagram is also consistent with experiments by Asanuma et al. (2008), and data from that study are added in Fig. 7 with open circles. It should be pointed out, however, that subsequent experimental studies were not able to observe fcc (Lin et al., 2009; Kuwayama et al., 2009).

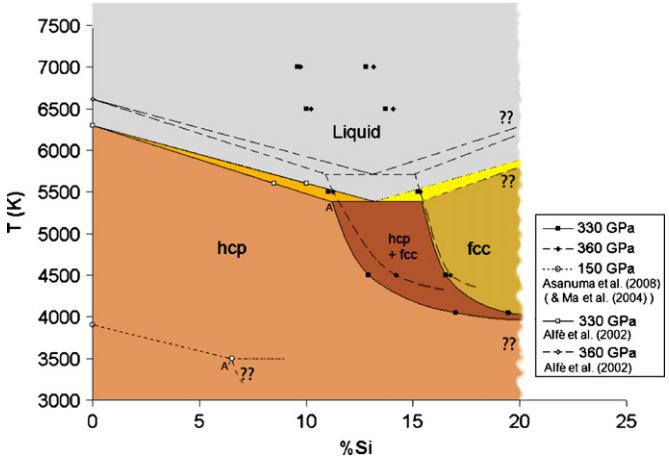

Fig. 7. Compositional phase diagram for the Fe–Si system (at.%) at the inner core boundary pressure (330 GPa). Superimposed with dashed lines is the same diagram for the centre of the core (360 GPa). The fcc and hcp coexisting compositions were calculated in this study (see text). The open circles, at 150 GPa, were derived from the study of Asanuma et al. (2008). Equivalent points with that study are marked with A and A′. The open squares and open diamond are taken from the ab initio data of Alfè et al. (2002).

4. Discussion

Earlier ab initio finite temperature molecular dynamics calculations using the technique of thermodynamic integration to calculate free energies (Vočadlo et al., 2003) showed that the thermodynamically stable phase of pure iron at core conditions is the hcp phase. This study confirms that result. Earlier ab initio studies also showed that light elements act to decrease the free energy difference bcc and hcp, but these were only performed at 0 K, and hcp still remained the stable phase (Côté et al., 2008a,b). It was, however, hypothesised that the combination of high temperature and light elements may be sufficient to make either bcc or fcc stable over the hcp phase. This is what we have tested here. We find that at a concentration of ~7 wt.% silicon, the combination of high temperatures (over 4000 K) and light element enrichment act to make the fcc phase thermodynamically stable at core conditions. hcp remains the stable phase at lower pressures and temperatures, as seen in a recent experimental study by Lin et al. (2009) where they used a concentration of ~8 wt.% silicon and reached pressures of 240 GPa and temperatures of 3000 K. We also find that the bcc structure becomes vibrationally stable as more light elements are added, so depending on the concentration of the alloying element and the effect of anharmonicity, it cannot be discarded as an inner core phase.

The light element concentration is generally thought to be about 4 wt.% (7.7 at.%) for the inner core and about 10 wt.% (18.1 at.%) for the outer core (Lin et al., 2002; Badro et al., 2007; Chen et al., 2008). First of all, Fig. 7 shows that even if Si was the only light element in the inner core, a composition of ~8 at.% places the inner core firmly in the hcp-field. The fcc phase does not become stable until the concentration of Si reaches 11 at.%. Secondly, the higher concentration of light element in the outer core could mean that the core is crystallising fcc and hcp at the eutectic. However, this would predict an inner composition that would be too high. Taken at face value, Fig. 7 predicts that the inner core must be in the hcp phase and that fcc is not stable. However, this phase diagram is for two com-

ponents only. The other light elements are also known to stabilise bcc, so they may also stabilise fcc. If so, the width of the two-phase region could widen, and it only needs to widen by ~3 at.% for the inner core to enter the two-phase field. This is supported by the results of Lao and Cohen (presented at APS, 2009) who also showed that nickel (Ni) also strongly stabilises the fcc phase, and pushes the core into the two-phase region. We suggest, therefore, that the inner core may exist in the two-phase region, with hcp and fcc coexisting throughout the core. The phase diagram also shows that the proportion of fcc to hcp changes slightly with temperature; the deeper inner core may, therefore, contain a greater proportion of fcc that the shallower inner core.

Finally, the S-wave velocity of the inner core is known to be less than that of all possible candidate phases, including the effect of light elements; this motivated Vočadlo (2007) to suggest that the inner core contains a small fraction of partial melt. However, the coexistence of fcc and hcp may allow the elastic velocities to be reduced via the mechanism proposed by Li and Weidner (2008) for the Earth's mantle. Li and Weidner showed that P-wave velocities of a material will be significantly lowered if the pressure increase during the passage of the wave causes a small amount of the material to transform from one phase to another. When the two phases are coexisting, this can be a very efficient process, as they showed for the olivine to wadsleyite transition. Although Li and Weidner demonstrated this for compressional waves, shear waves should have an analogous, and potentially larger effect. This mechanism may well occur between fcc and hcp during the passage of a seismic wave in the inner core, effectively reducing the velocity from its elastic, unrelaxed values, and explaining the low observed S-wave velocities in the inner core.

Acknowledgements

The work of ASC was supported by NERC grant NE/C519662/1. The computations were performed on the HECToR service.

References

Alfè, D., Gillan, M.J., Price, G.D., 2000a. Constraints on the composition of the Earth's core from ab initio calculations. Nature 401, 462–464.
Alfè, D., Gillan, M.J., Price, G.D., 2000b. Composition and temperature of the Earth's core constrained by combining ab initio calculations and seismic data. Earth Planet. Sci. Lett. 195, 91–98.
Alfè, D., Price, G.D., Gillan, M.J., 2001. Thermodynamics of hexagonal close packed iron under Earth's core conditions. Phys. Rev. B 64, 04512316.
Alfè, D., Gillan, M.J., Price, G.D., 2002. Composition and temperature of the Earth's core constrained by combining ab initio calculations and seismic data. Earth Planet. Sci. Lett. 195, 91–98.
Alfè, D., 2009. PHON: A program to calculate phonons using the small displacement method. Computer Physics Communication, doi:10.1016/j.cpc.2009.03.010.(program available at http://chianti.geol.ucl.ac.uk/~dario).
Anderson, O.L., 1985. Ramsey's silicate core revisited. Nature 314, 407–408.
Andrault, D., Fiquet, G., Kunz, M., Visocekas, F., Haussermann, D., 1997. The orthorhombic structure of iron: an in situ study at high temperature and high pressure. Science 278, 831–834.
Asanuma, H., Ohtani, J., Sakai, T., Terasaki, H., Kamada, S., Hirao, N., Sata, N., Ohishi, Y., 2008. Phase relations of Fe–Si alloy up to core conditions: implications for the Earth's inner core. Geophys. Res. Lett. 35, L12307.
Badro, J., Fiquet, G., Guyot, F., Gregoryanz, E., Occelli, F., Antonangeli, D., d'Astuto, M., 2007. Effect of light elements on the sound velocities in solid iron: implications for the composition of Earth's core. Earth Planet. Sci. Lett. 254, 233–238.
Belonoshko, A.B., Ahuja, R., Johansson, J., 2003. Stability of the body-centred-cubic phase of iron in the Earth's inner core. Nature 424, 1032–1034.
Belonoshko, A.B., Skorodumova, N., Rosengren, A., Johansson, B., 2008. Elastic anisotropy of Earth's inner core. Science 319, 797–800.
Blöchl, P.E., 1994. Projector augmented-wave method. Phys. Rev. B 50, 17953–17979.
Boehler, R., 1986. The phase diagram of iron to 430 kbar. Geophys. Res. Lett. 13, 1153–1156.
Chen, B., Gao, L., Funakoshi, K., Li, J., 2008. Thermal expansion of iron-rich alloys and implications for the Earth's core. PNAS 104 (22), 9162–9167.
Côté, A.S., Vočadlo, L., Brodholt, J.P., 2008a. Light elements in the core: effects of impurities on the phase diagram of iron. Geophys. Res. Lett. 35, L05306.
Côté, A.S., Vočadlo, L., Brodholt, J.P., 2008b. The effect of silicon impurities on the phase diagram of iron and possible implications for the Earth's core structure. J. Phys. Chem. Solid 69, 2177–2181.
Dobson, D.P., Vočadlo, L., Wood, I.G., 2002. A new high-pressure phase of FeSi. Am. Mineral. 87, 784–787.
Dubrovinsky, L., 2007. Body-centred cubic iron-nickel alloy in Earth's core. Science 316, 1880–1883.
Kresse, G., Furthmuller, J., 1996. Efficient iterative schemes for ab initio total-energy calculations using a plane-wave basis set. Phys. Rev. B 54, 11169–11186.
Kuwayama, Y., Sawai, T., Hirose, K., Nagayoshi, S., Ohishi, Y., 2009. Phase relations of iron-silicon alloys at high pressure and high temperature. Phys. Chem. Miner., doi:10.1007/s00269-009-0296-0.
Li, L., Weidner, D., 2008. Effect of phase transitions on compressional-wave velocities in the Earth's mantle. Nature 454, 984–986.
Lin, J.-F., Heinz, D.L., Campbell, A.J., Devine, J.M., Shen, G.Y., 2002. Iron–silicon alloy in the Earth's core? Science 295, 313–315.
Lin, J.-F., Scott, H.P., Fischer, R.A., Chang, Y.-Y., Kantor, I., Prakapenka, V., 2009. Phase relations of Fe–Si alloy in the Earth's core. Geophys. Res. Lett. 36, L06306.
Saxena, S.K., Shen, G., Lazor, P., 1993. Experimental evidence for a new iron phase and implications for the Earth's core. Science 260, 1312–1314.
Saxena, S.K., Dubrovinsky, L.S., 2000. Iron phases at high pressures and temperatures: phase transition and melting. Am. Mineral. 85, 372–375.
Söderlind, P., Moriarty, J.A., Wills, J.M., 1996. First-principles theory of iron up to earth-core pressures: structural, vibrational, and elastic properties. Phys. Rev. B 53, 14063–14072.
Stixrude, L., Cohen, R.E., 1995. Constraints on the crystalline structure of the inner core: mechanical instability of BCC iron at high pressure. Geophys. Res. Lett. 22, 125–128.
Stixrude, L., Cohen, R.E., Singh, D.J., 1994. Iron at high pressure: linearized-augmented-plane-wave computations in the generalized-gradient approximation. Phys. Rev. B 50, 6442–6445.
Vočadlo, L., de Wijs, G.A., Kresse, G., Gillan, M.J., Price, G.D., 1997. First principles calculations on crystalline and liquid iron at Earth's core conditions. Faraday Discuss. 106, 205–217.
Vočadlo, L., Brodholt, J., Alfe, D., Price, G.D., Gillan, M.J., 1999. The structure of iron under the conditions of the Earth's inner core. Geophys. Res. Lett. 26, 1231–1234.
Vočadlo, L., Alfè, D., Gillan, M.J., Wood, I.G., Brodholt, J.P., Price, G.D., 2003. Possible thermal and chemical stabilization of body centred-cubic iron in the Earth's core. Nature 424, 536–539.
Vočadlo, L., 2007. Ab initio calculations of the elasticity of iron and iron alloys at inner core conditions: evidence for a partially molten inner core? Earth Planet. Sci. Lett. 254, 227–232.
Vočadlo, L., Wood, I.G., Alfè, D., 2008. Ab initio calculations on the free energy and high P–T elasticity of face-centred-cubic iron. Earth Planet. Sci. Lett. 268, 444–449.
Wang, Y., Perdew, J., 1991. Correlation hole of the spin-polarized electron gas, with exact small-wave-vector and high-density scaling. Phys. Rev. B 44, 13298–13307.